Soft Matter

PAPER

Zwitterionic surfactant/cyclodextrin hydrogel: microtubes and multiple responses†

Lingxiang Jiang, Yun Yan and Jianbin Huang*

Previously reported polymer-free cyclodextrin (CD) hydrogels usually relied on tailored modification of CDs or careful design and synthesis of guests, which may limit their mass production or application. Herein, we report on a hydrogel system based on a native CD (β-CD) and a commercially available zwitterionic surfactant (tetradecyl dimethylammonium propane sulfonate, TDPS). The TDPS/β-CD hydrogel shows excellent mechanical properties with an elastic modulus $>10 \times 10^4$ Pa and yield stress >100 Pa. Microstructures in the hydrogel were identified to be well-defined microtubes, featuring a long, flexible, bundling, and entangling nature. The microtubes form an extensive 3D network and then a strong hydrogel. The building unit of the microtubes was determined to be 2TDPS@3β-CD complex, which forms a 3D array with a considerable crystalline nature. The array eventually folds up into the microtubes. In addition, the TDPS/β-CD hydrogel was found to be multi-responsive to temperature, pH, urea, and a competitive guest. It is envisioned that the commercial availability and low cost of β-CD and TDPS may facilitate the mass production and application of the present TDPS/β-CD hydrogel.

1 Introduction

Polysaccharide-based self-assemblies are a class of promising materials in terms of rich functionality, bio-compatibility, structural robustness,[1] and wide-spread applications from food/cosmetics processing[2] to tissue engineering.[3] In particular, hydrogels composed of cyclodextrins[4] CDs, (as shown in Fig. 1, a series of donut-like oligosaccharides with hydrophobic cavities and a hydrophilic outer surface) draw continually increasing attention, not only because of CDs' saccharide nature, but also arising from their ability to include a wide variety of guest molecules.[5] Such inclusion ability endows CD hydrogels with a number of unique opportunities (not easily accessible by other gel systems).[6] For instance, the well-established host–guest chemistry of CDs can be utilized to build up and break down gel structures, introduce responsive functionalities, or enhance selectivity in applications such as catalysis and extraction.[7]

The reported CD-based hydrogel systems can be generally divided into two classes. One class involves polymers, where the gelation largely relies on the polymer scaffold.[8] For example, polyrotaxanes of α-CD on polyethylene glycol with $M_w > 2000$ were reported to be hydrogelators;[9] CDs can be polymerized by cross linkers or be grafted onto polymer bones to gel water.[10] The other class is polymer-free, in which the gelation depends on subtly controlled intermolecular interactions between small molecules.[11] Successful control of the interactions is usually achieved by tailored modification of CDs, or careful design and synthesis of guests, or both. For example, several functionalized β-CDs were reported to form self-inclusion complexes,[12] which
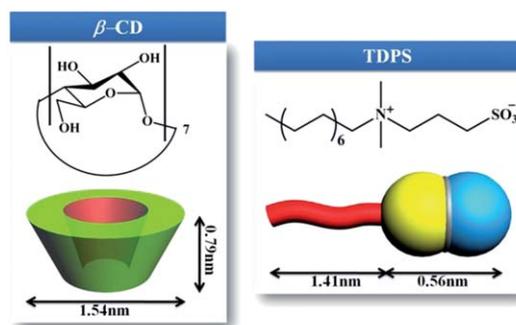

Fig. 1 Molecular structures, 3D illustrations, and molecular sizes of β-CD and TDPS. For β-CD, the hydrophobic cavity and hydrophilic exterior are denoted by crimson and green, respectively. For TDPS, the C14 tail, ammonium group, and sulfonate group are represented by red line, yellow hemisphere, and blue hemisphere, respectively. Molecular sizes are marked on double arrows, where those of β-CD are taken from literature[4c] and those of TDPS are calculated using CPK model. Please note that the 3D illustrations are not scaled according to the molecular sizes.

Beijing National Laboratory for Molecular Sciences (BNLMS), State Key Laboratory for Structural Chemistry of Unstable and Stable Species, College of Chemistry and Molecular Engineering, Peking University, Beijing, 100871, P. R. China. E-mail: jbhuang@pku.edu.cn

act as supramolecular polymers to gel water; complexes between α-CD and a special kind of amphiphile were found to be hydrogel-forming,[13] in virtue of CD–CD H-bonds and intermolecular contact between two end groups on the amphiphiles. However, mass production or application of these CD hydrogels would be limited by the high cost or time-consuming, complicated synthesis. In this context, it is desirable to develop a new CD hydrogel system, which is based on native CDs and commercially available guests.

Recently, it was reported by us[14] that a SDS@2β-CD complex (SDS is an anionic surfactant) is able to self-assemble into lamellae, microtubes, and vesicles at different concentrations in aqueous solution, although surfactant/CD complexes were previously believed to be quite soluble and unaggregatable in water because of the hydrophilic outer surface. The self-assembly of SDS@2β-CD complex was proposed to be driven by CD–CD H-bonds and to be mediated by electrostatic repulsion between SDS headgroups. It seemed to us that, among the three kinds of SDS@2β-CD aggregates, the microtubes could be a good candidate for hydrogel formation. However, the microtube suspension was found to be a viscous fluid but not a hydrogel.[14a] The failure in hydrogel formation is understandable if one considers the following facts: 1) the microtubes are strongly electrostatically repulsive to each other, incapable of bundling or entangling together to form a 3D network, and 2) the microtubes are brittle and inflexible, and will be broken into shorter ones other than elastically deformed under shear. We reason that the strong electrostatic repulsion between SDS headgroups is responsible for the two facts and eventually results in fluidity of the system. Therefore, it is assumed that hydrogel formation may be enabled by reducing the repulsion between surfactant headgroups.

Herein, we report on a hydrogel system based on a β-CD/TDPS complex, in which TDPS (tetradecyl dimethylammonium propane sulfonate, Fig. 1) is a commercially available zwitterionic surfactant. The hydrogel is of good mechanical performance with yield stress >100 Pa and elastic modulus >10 × 10⁴ Pa. The hydrogel is dominated by well-defined microtubes (diameter ~300 nm, wall thickness ~40 nm) with several gel-forming features including bundling, entangling, and flexibility. The difference between the TDPS/β-CD and SDS@2β-CD microtubes possibly originates from the minimized repulsion between the zwitterionic headgroups of TDPS. The structure of the TDPS/β-CD microtubes is resolved on a molecular level. Moreover, multiple responses of the TDPS/β-CD hydrogel to temperature, pH, urea, and competitive guests are investigated.

2 Experimental section

2.1 Materials

Tetradecyl dimethylammonium propane sulfonate (TDPS) was purchased from Sigma-Aldrich and was used as received. β-Cyclodextrin (β-CD) was purchased from Sinopharm Chemical Reagent Co. with a water content of 14%. Adamantane-1-carboxylic acid (Ada-CA) was purchased from Alfa Aesar and was used as received. Water (H₂O) was redistilled from potassium permanganate. All the other reagents are of AR grade.

2.2 Microscopy

Samples were observed by optical microscopy (Leica), field emission-scanning electronic microscopy (FE-SEM, Hitachi S4800, 1 kV), transmission electronic microscopy (TEM, Jeol JEM 100CX, 80 kV), and atomic force microscopy (AFM, Nanoscope IIIa). Before FE-SEM observation, the samples were mounted onto a silicon wafer and were then dried by N₂ flow. Before TEM observation, the samples (without staining) were transferred onto a copper grid (230 meshes) and were allowed to dry. In AFM analyses, the samples were transferred to the freshly cleaved mica; the sample-loaded mica was dried by N₂ flow and was then examined by AFM in tapping mode.

2.3 Rheology

Rheological properties were measured by a Thermo Haake RS300 rheometer with cone and plate geometry (35 mm diameter, 0.105 mm cone gap). The temperature was kept at 25 °C and a water trap was used to minimize water evaporation from the sample. Frequency spectra were conducted in the linear viscoelastic regime of the samples determined from dynamic strain sweep measurements.

2.4 Small- and wide-angle X-ray scattering (SAXS and WAXS)

Measurements were performed by a highflux SAXSess (Anton-Paar, Austria, Cu-Kα, λ = 0.154 nm), equipped with a Kratky block-collimation system and an imaging plate (IP) as the detector. Both SAXS and WAXS scattering profiles can be simultaneously recorded. The scattering peak positions were calibrated with silicon powder for the wide-angle region and silver behenate for the small-angle region. A temperature control unit (Anton-Paar TCS-120) in conjunction with the SAXSess was utilized to control the temperature at 25 °C. Samples were loaded into a quartz capillary with a diameter of 1 mm. An exposure time of 15 mins was found to be long enough to give a good signal-to-noise ratio. The scattering curve of pure water filled in the same capillary was recorded as the background.

3 Results and discussion

3.1 Phase behavior of TDPS/β-CD/water system

For sample preparation, the desired amounts of TDPS, β-CD, and water were weighed into tubes; the samples were heated to obtain transparent, isotropic solutions; the solutions were then thermostatically incubated at 25 °C (at least 3 days) to allow precipitation or gelation. The investigated TDPS:β-CD ratio ranges from 0.3 to 1.2, and the investigated CD concentration covers a board range from 5 to 50 wt% (Fig. 2a).

On the basis of observations by the naked eye and by optical microscopy, the phase diagram of the TDPS/β-CD system is divided into 5 regions, assigned as Regions I to V from left to right along the ratio axis (Fig. 2a). In Region I, solid precipitates can be found in the tube bottom (Fig. 2b, I) and the precipitates were determined to be flake crystals (Fig. 3a). In Region II, solid precipitates coexist with a viscous, turbid suspension, as demonstrated by Fig. 2b, II, where the interface
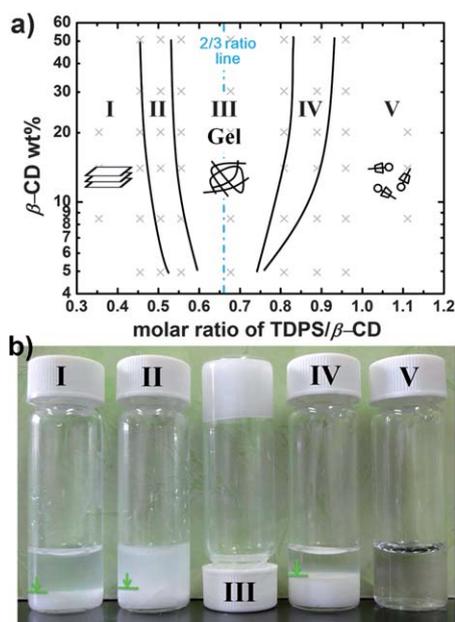
Fig. 2 A phase diagram of the TDPS/β-CD/water system (a). Photographs of 5 samples in different regions (b), where the β-CD concentration is 8.5 wt% for all the 5 samples and ratios are 0.45 (**I**), 0.55 (**II**), 0.67 (**III**), 0.85 (**IV**), and 0.95 (**V**). The sample in Region **III** is a hydrogel that can stand against its own weight in an inverted tube.
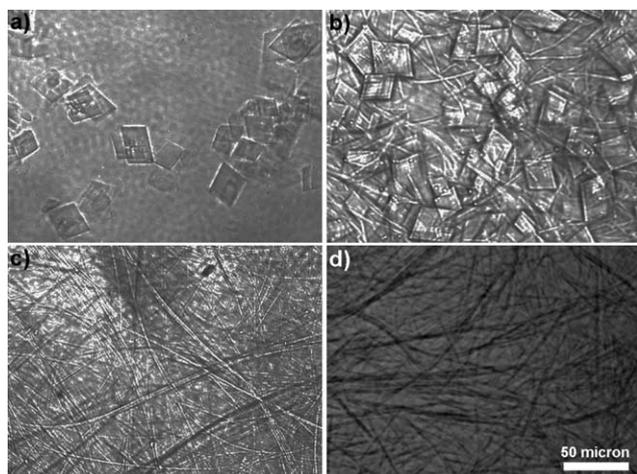

Fig. 3 Optical microscopy images for TDPS/β-CD samples in Regions **I** (a), **II** (b), **III** (c), and **IV** (d). The four images share the same scale bar.

(not very clear) is highlighted by a green line. The microstructures therein are flake crystals and fibers (Fig. 3b), where the latter probably accounts for the viscosity and turbidity of the suspension. In Region **III**, the samples are uniform, opalescent hydrogels that can stand their own weight in inverted tubes (Fig. 2b, **III**). The hydrogel is dominated exclusively by a large amount of long (in the order of sub-millimetre), flexible, and entangled fibers (Fig. 3c). In Region **IV**, the samples, after been cooled down to 25 °C, first appear as uniform hydrogels but then separate into a transparent solution (upper phase) and a hydrogel (bottom phase), as shown in Fig. 2b, **IV**. The microstructure in the bottom phase (Fig. 3d) is similar to that in

Region **III**. In Region **V**, the samples are clear solutions (Fig. 2b, **V**).

It is noteworthy that the precipitation (Regions **I** and **II**) dominates the system with TDPS : β-CD ratios close to 1 : 2, that the hydrogel and fibers (Region **III**) prevail in the system with ratios around 2 : 3, and that the clear solution (Regions **IV** and **V**) appears (or partly appears) with ratios near 1 : 1. The present work focuses on Region **III** where a uniform hydrogel forms. The fact that the hydrogel region is centered along the 2 : 3 ratio line implies that the 2 : 3 ratio may play an important role in gelation (will be discussed in Section 3.3). Most measurements in this work were conducted on one specific hydrogel sample in Region **III** (TDPS : β-CD = 2 : 3, β-CD 8.5 wt%). As for the other four regions, our preliminary results suggest that the flake crystals in Regions **I** and **II** might come from TDPS : β-CD 2 : 1 complex, and that the clear solution in Regions **IV** and **V** may contain unaggregated TDPS : β-CD 1 : 1 complex as well as TDPS micelles. Further investigation into these four regions is beyond the scope of this work.

3.2 Rheological properties and microstructures of TDPS/β-CD hydrogel

The rheological properties of the TDPS/β-CD hydrogel were assessed by dynamic rheology measurements. In these measurements, the hydrogel sample was deformed sinusoidally with frequency f to give the elastic (or storage) modulus G' and viscous (or loss) modulus G''. During the oscillation frequency sweep test, the stress was chosen as 1 Pa (much lower than the yield value, see below) to be nondestructive to the gel structure and the frequency was varied exponentially. As Fig. 4a shows, both G' and G'' are basically independent of the frequency, while G' ($\sim 1 \times 10^4$ Pa) is dominating the G'' (~ 300 Pa) over the entire investigated frequency range. The frequency sweep result indicates a typical solid-like rheological behavior for the hydrogel. During the amplitude sweep test, the frequency f was kept at 1 Hz, and the applied stress was elevated exponentially. As plotted in Fig. 4b, below a certain stress (see the arrow), G' and G'' is independent of the stress and the deformation is always close to 0, which infers that the gel structure is kept completely intact. Beyond a certain stress, G' and G'' drop dramatically and the sample is deformed to a great extent ($\sim 160\%$), suggesting that the gel structure is destructed (or yielded). The stress, ~ 150 Pa, is denoted as the yield point of the hydrogel. As shown by the photograph (Fig. 4c), this yield stress is high enough not only to stand hydrogel's own weight but even to hold the weight of an
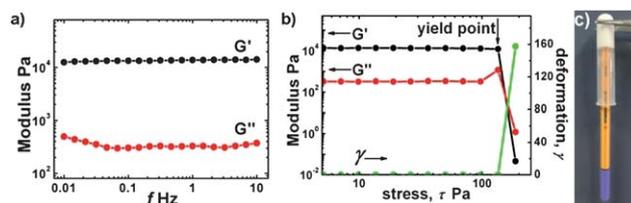

Fig. 4 Dynamic rheology profiles of the TDPS/β-CD hydrogel in oscillation frequency sweep mode (a) and in amplitude sweep mode (b). A photograph showing that the hydrogel is strong enough to hold an embedded pen (c).

embedded pen. As reflected by the above results, the TDPS/β-CD hydrogel exhibits excellent mechanical performance.

For microstructures of the TDPS/β-CD hydrogel, several mutual complementary microscopy techniques were employed, including field emission-scanning electronic microscopy (FE-SEM), transmission electronic microscopy (TEM), and atomic force microscopy (AFM). For FE-SEM observation, the hydrogel sample was mounted onto a silicon wafer and was then dried by N_2 flow. Fig. 5a shows a FE-SEM image, where plenty of fibers (longer than tens of microns) and their bundles prevail in the entire scope. As for TEM observation, the hydrogel sample (without staining) was transferred onto a copper grid and was air-dried. TEM images were given in Fig. 5b–5e with different magnifications. In Fig. 5b, a 3D network structure can clearly be seen, which is made of single strings of fibers as well as bundles of them. It is manifest in Fig. 5c–2e that each single string of fiber is a hollow microtube with diameters from 200 to 400 nm and wall thicknesses from 30 to 50 nm.

In AFM analyses, the hydrogel sample was transferred to the freshly cleaved mica; the sample-loaded mica was dried by N_2 flow and was then examined by AFM in tapping mode. AFM measurements generally give long tape-like structures with height far smaller than width. These tapes presumably originate from hollow microtubes, which collapsed as a result of the loss of inner water during the drying process. A single tape is shown in Fig. 6, including a height map, a reconstructed 3D plot, and a sectional analysis. Clearly, this tape is of ~500 nm width and ~60 nm height. The width of ~500 nm is larger than the diameters observed by TEM (200 to 400 nm), which is understandable considering the broadening effect of AFM tips. The height of ~60 nm corresponds to a wall thickness of ~30 nm for a micro-tube, in consistent with that from TEM observation (30 to 50 nm). The AFM results further confirm a tubular structure for the fibers.

Combining the results from different microscopy techniques, one can find that the TDPS/β-CD microtubes are long, flexible,
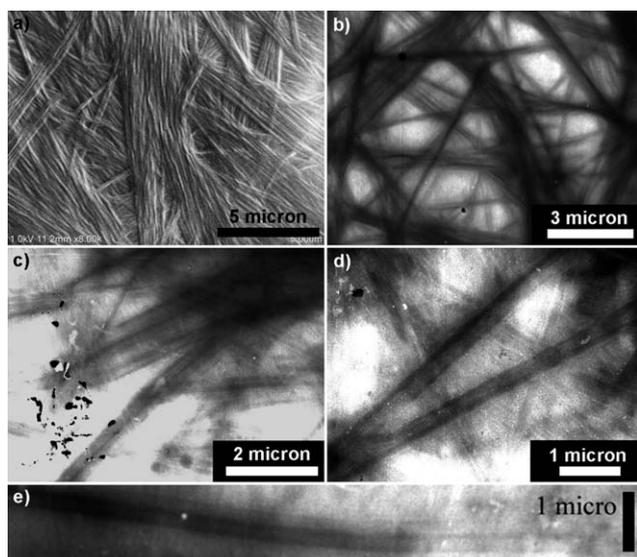

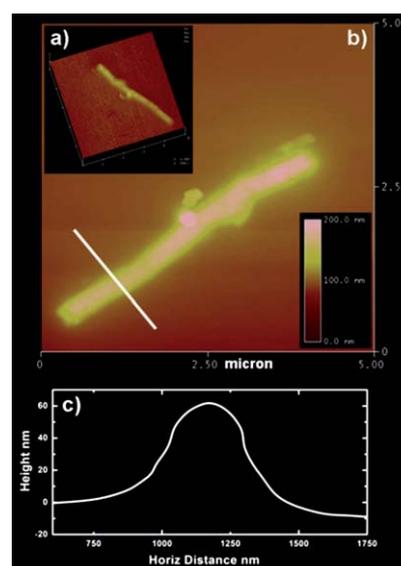**Fig. 6** AFM results of the TDPS/β-CD hydrogel: the reconstructed 3D plot (a), the height map (b), and the sectional analysis (c).

bundling, and entangling, in great contrast to the previously reported SDS@2β-CD microtubes.[14a] These features enable the TDPS/β-CD microtubes to form an extensive 3D network (like Fig. 5b) that can sustain (or deform elastically) under high stress (even over 100 Pa), whereas the SDS@2β-CD microtube suspension is fluid under stress. We reason that the zwitterionic headgroup of TDPS (over the anionic headgroup of SDS) is responsible for the difference between the two kinds of micro-tubes. In the case of SDS@2β-CD microtubes, the microtube surface (covered by the anionic headgroups) is highly negatively charged, prohibiting the microtubes from bundling or entan-gling; the electrostatic repulsion between SDS@2β-CD complexes inside a single microtube leads to a high inner tension, making the microtubes brittle, inflexible, and unable to deform elastically. As for the TDPS/β-CD microtubes, those undesirable effects for gel formation are avoided because the electrostatic repulsion is minimized by the zwitterionic head-group of TDPS.

3.3 Structure of the TDPS/β-CD microtubes on a molecular level

Given the molecular structures of TDPS and β-CD (Fig. 1), their complexes are able to adopt several conformations depending on different conditions. 1) TDPS@β-CD, where the TDPS tail is threaded through one CD cavity (Fig. 7a). Such a conformation is preferred in an aqueous solution with equal molarities of TDPS and β-CD. 2) TDPS@2β-CD, in which the TDPS tail is covered by two CD donuts (Fig. 7a). This conformation is favored in an aqueous solution with 1 : 2 molarities of TDPS and β-CD. 3) 2TDPS@3β-CD, where two TDPS tails are threaded through three CD cavities, leaving two TDPS headgroups oppositely facing (Fig. 7a). This conformation is not likely to exist in a free (unaggregated) state in solution because the attraction between the two TDPS tails is not strong enough to resist molecular thermal motion, but the 2TDPS@3β-CD
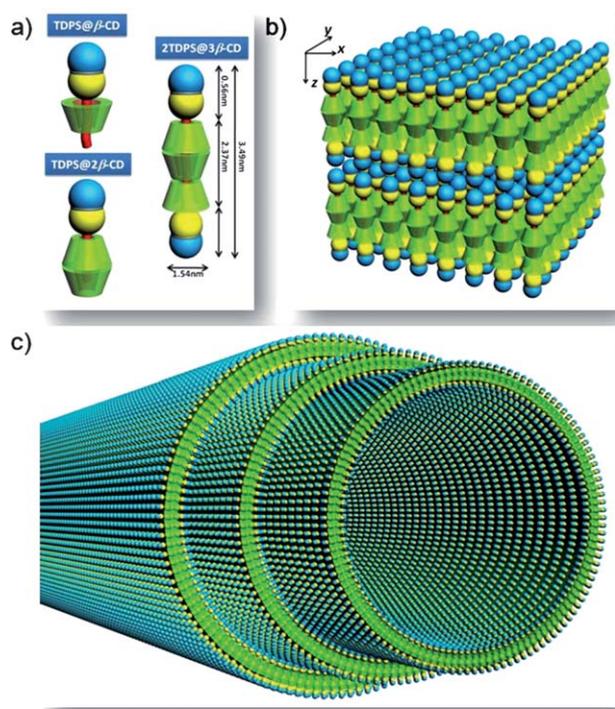

Fig. 5 FE-SEM (a) and TEM (b–e, in different magnifications) images of the TDPS/β-CD hydrogel.

Fig. 7 Schematic illustrations of different TDPS/β-CD complexes (a), an array of the 2TDPS@3β-CD complex (b), and a microtube of the 2TDPS@3β-CD complex (c). Please note that the mutual directions of CDs in TDPS@2β-CD and 2TDPS@3β-CD complexes are not experimentally determined. Nevertheless, it is generally believed that the head-to-tail alignment of CDs is energetically favored because the CD–CD H-bonds are maximized in such an alignment. Please note that the 3D illustrations are not scaled according to the molecular sizes.

conformation may emerge in a restricted space, such as crystals or microtubes in our case. Now a question arises as to which kind of TDPS/β-CD complex is the building unit of the microtubes. This question is addressed by phase diagram analysis, proton nuclear magnetic resonance (^{1}H-NMR), and electron spraying ionization mass spectrometry (ESI-MS).

As we stated in Section 3.1, the TDPS : β-CD 1 : 2 and 1 : 1 ratios correspond to precipitate formation and clear solution, respectively, while the 2 : 3 ratio corresponds to microtubes and gel formation. It is suggested that both TDPS@2β-CD and TDPS@β-CD complexes are in capable of forming microtubes or gels, and we thus propose 2TDPS@3β-CD complex as the building unit for the microtubes.

This proposition is first supported by confirming a TDPS : β-CD 2 : 3 ratio in the microtubes. Please note that the TDPS : β-CD ratio within the microtubes is not necessarily the same as the prepared 2 : 3 ratio. The ratio inside the microtubes is accessed by ^{1}H-NMR measurements using the following procedue.[15] Considering a general gel composed of, say, gelator **1**, where **1** exists both in free (unaggregated) and in gelled states. First, in ^{1}H-NMR experiments of the gel, the proton signal is sharp and clear for free **1** in solution, whereas that is broadened beyond detection for gelled **1** because of the extremely long relaxation time. The concentration of free **1** can thus be determined by integrating the observable proton signal of **1** (with

respect to an internal reference). Next, the gel is destroyed (for example by adding acid or base to a pH-sensitive gel) to release all of the gelled **1**. NMR measurements of this destroyed gel can give the total concentration of **1** (with respect to the internal reference). A simple subtraction then leads to the fraction of gelled **1**. In our case, it is straightforward to employ the above procedure to measure the TDPS : β-CD ratio in the gelled state (*i.e.*, in the microtubes), where 1 wt% DMSO was chosen as the internal reference and the gel was destroyed by addition of 100 mM NaOH (for the reason why NaOH would destroy the gel, please see Section 3.4). NMR spectra of the TDPS/β-CD hydrogel and the destroyed one are shown in Figure S1 (please see the ESI†), giving a TDPS : β-CD 2 : 3 ratio within the microtubes.

The 2TDPS@3β-CD proposition is further supported by ESI-MS (in positive mode) results. In Figure S2 (please see the ESI†), a peak for $[2TDPS + 3β\text{-}CD + 2Na]^{2+}$ ($m/z = 2088.1$) is observable, suggesting the possible existence of the 2TDPS@3β-CD complex in the microtubes. Moreover, the sizes of the 2TDPS@3β-CD complex fit the postulated crystal structure well, as will be discussed below.

The arrangement of the 2TDPS@3β-CD building units in the microtubes is resolved by small-angle X-ray scattering and wide-angle X-ray scattering (SAXS–WAXS, *in situ* measurement in the hydrate state). As show in Fig. 8, the SAXS–WAXS profile is characterized by many Bragger diffraction peaks. The sharpness of the Bragger peaks indicates that the microtubes are of considerable cystalline nature. These peaks can be divided into 5 sets with regular spacings (Fig. 8). Although these repeat distance d (or d-spacing) data do not allow resolving the crystal structure of the microtubes on the atomic scale (limited by its multi-crystal origin), insights into the structure can be gained by comparing
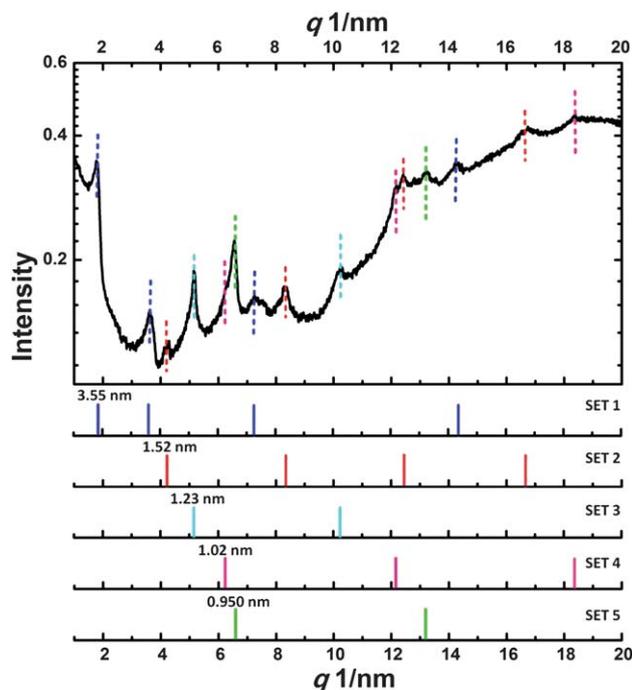

Fig. 8 The SAXS–WAXS profile of the TDPS/β-CD hydrogel.

the *d*-spacings with sizes of the 2TDPS@3β-CD complex. Roughly speaking, the complex is ∼3.49 nm long and ∼1.54 nm wide. Given the above structural data, we postulate a crystal structure with $a = c = 1.67$ nm, $b = 3.55$ nm, $\alpha = \gamma = 90°$, and $\beta = 133°$. On one hand, these parameters are reasonable for the sizes of the 2TDPS@3β-CD complex, where b (∼3.55 nm) is close to the complex height (∼3.49 nm) and a and c (1.67 nm) are slightly larger than the complex width (∼1.54 nm). On the other hand, the diffraction peaks predicted from the postulated structure are in satisfactory consistency with the measured ones (Table 1).

An array of the 2TDPS@3β-CD complex is illustrated in Fig. 7b, according to the postulated crystal structure. By comparing this array to that of the SDS@2β-CD complex, one can identify their similarity and difference. In the *xy* plane, both 2TDPS@3β-CD and SDS@2β-CD complexes form lamellae allowing the formation of an extensive lateral network of CD–CD H-bonds. Along the *z* axis, the SDS@2β-CD lamellae keep a large distance (several tens of nm) from each other due to electrostatic repulsion between anionic headgroups, but the 2TDPS@3β-CD lamellae stack together due to the absence of electrostatic repulsion between zwitterionic headgroups. At last, the 2TDPS@3β-CD array scrolls up in the *z* direction into the final microtubes (Fig. 7c).

3.4 Multiple responses of the TDPS/β-CD hydrogel

It is well established that the physical and chemical properties of cyclodextrins are responsive to multiple external stimuli such as temperature, pH, and different guests. Therefore, the present CD-based hydrogel is expected to be inherently multi-responsive. 1) Temperature. When heated to above the gelation temperature (∼35 °C), the opalescent hydrogel turns into a transparent solution (Figure S3a, please see the ESI†), resulting from an increase of solubility of the TDPS/β-CD complex. Such a temperature-induced transition is reversible. 2) pH. In response to NaOH addition, the opalescent hydrogel becomes a clear solution at pH ∼12 (Figure S3b, please see the ESI†), which is close to the pK_a of β-CD, 12.2. The ionization of β-CD at high pH would significantly destabilize the 2TDPS@3β-CD complex and the microtubes due to electrostatic repulsion as well as the disappearance of CD–CD H-bonds. 3) Urea. The addition of 2 M urea will alter the TDPS/β-CD hydrogel into a clear solution, likely because of the breakage of the CD–CD H-bonds. 4) Ada-CA (adamantane-1-carboxylic acid, a strongly competitive guest for β-CD). The addition of 200 mM Ada-CA gives rise to precipitation out from the TDPS/β-CD. It is anticipated this TDPS/β-CD hydrogel is also responsive to other kinds of β-CD guests.

Table 1 Comparison between the measured and predicted *d*-spacings

Set	*h.k.l*	Measured *d*(nm)	Predicted *d*(nm)
1	0.1.0	3.55	3.55
2	−1.1.0	1.52	1.53
3	1.0.0	1.23	1.23
4	0.1.1	1.02	1.02
5	1.1.0	0.95	0.95

Conclusions

In conclusion, we have achieved a kind of CD-based hydrogel by employing a native CD (β-CD) and a zwitterionic surfactant (TDPS). The TDPS/β-CD hydrogel shown excellent mechanical properties with elastic modulus $>10 \times 10^4$ Pa and yield stress >100 Pa (high enough to hold the weight of an embedded pen). Microstructures in the hydrogel were identified to be well-defined microtubes. These TDPS/β-CD microtubes are long, flexible, bundling, and entangling (in great contrast to the previously reported SDS@2β-CD microtubes), and they can thus form an extensive 3D network and eventually a strong hydrogel. Differences between the TDPS/β-CD and SDS@2β-CD microtubes are attributed to the surfactant headgroups: zwitterionic for TDPS (electrostatic repulsion minimized) and anionic for SDS (highly electrostatically repulsive). The building unit of the TDPS/β-CD microtubes was determined to be the 2TDPS@3β-CD complex. The complex laterally expands into lamellae, the lamellae stack together in the perpendicular direction to form a 3D array, and the array eventually folds up into the microtubes. Moreover, the present TDPS/β-CD hydrogel was found to be multi-responsive to temperature, pH, urea, and a competitive guest (Ada-CA).

Since both β-CD and TDPS are commercially available and cost-effective and the TDPS/β-CD hydrogel samples can be conveniently prepared, this hydrogel system is envisioned to be promising in mass production and application. In addition, the multi-responsive nature of the TDPS/β-CD hydrogel system allows further modification to broaden its applications.

Notes and references

1 (a) R. L. Whistler and C. L. Smart, *Polysaccharide Chemistry*, Academic Press, New York, 1953; (b) K. Akiyoshi, S. Deguchi, N. Moriguchi, S. Yamaguchi and J. Sunamoto, *Macromolecules*, 1993, **26**, 3062–3068; (c) N. Morimoto, F. M. Winnik and K. Akiyoshi, *Langmuir*, 2007, **23**, 217–223.
2 (a) W. Pilnik and F. M. Rombouts, *Carbohydr. Res.*, 1985, **142**, 93–105; (b) N. A. Peppas, J. Z. Hilt, A. Khademhosseini and R. Langer, *Adv. Mater.*, 2006, **18**, 1345–1360.
3 (a) J. L. Drury and D. J. Mooney, *Biomaterials*, 2003, **24**, 4337–4351; (b) S. Ladet, L. David and A. Domard, *Nature*, 2008, **452**, 76–80.
4 (a) A. Harada, J. Li and M. Kamachi, *Nature*, 1992, **356**, 325–327; (b) M. V. Rekharsky and Y. Inoue, *Chem. Rev.*, 1998, **98**, 1875–1918; (c) W. Saenger, J. Jacob, K. Gessler, T. Steiner, D. Hoffmann, H. Sanbe, K. Koizumi, S. M. Smith and T. Takaha, *Chem. Rev.*, 1998, **98**, 1787–1802; (d) H.-J. Schneider, F. Hacket and V. Rudiger, *Chem. Rev.*, 1998, **98**, 1755–1785.
5 (a) K. Ohga, Y. Takashima, H. Takahashi, Y. Kawaguchi, H. Yamaguchi and A. Harada, *Macromolecules*, 2005, **38**, 5897–5904; (b) M. Miyauchi, Y. Takashima, H. Yamaguchi and A. Harada, *J. Am. Chem. Soc.*, 2005, **127**, 2984–2989; (c) T. Ogoshi, Y. Takashima, H. Yamaguchi and A. Harada, *J. Am. Chem. Soc.*, 2007, **129**, 4878–4879.
6 J. W. Steed and J. A. Foster, *Angew. Chem., Int. Ed.*, 2010, **49**, 6718–6724.
7 (a) K. J. C. van Bommel, M. C. A. Stuart, B. L. Feringa and J. van Esch, *Org. Biomol. Chem.*, 2005, **3**, 2917–2920; (b) A. Ajayaghosh, V. K. Praveen, C. Vijayakumar and S. J. George, *Angew. Chem., Int. Ed.*, 2007, **46**, 6260–6265; (c) Z. Dzolic, M. Cametti, A. Dalla

Cort, L. Mandolini and M. Zinic, *Chem. Commun.*, 2007, 3535–3537; (*d*) F. Rodriguez-Llansola, J. F. Miravet and B. Escuder, *Chem. Commun.*, 2009, 7303–7305.

8 (*a*) D. Mocanu, D. Vizitiu and A. Carpov, *J. Bioact. Compat. Polym.*, 2001, **16**, 315–342; (*b*) F. van de Manakker, T. Vermonden, C. F. van Nostrum and W. E. Hennink, *Biomacromolecules*, 2009, **10**, 3157–3175.

9 J. Li, A. Harada and M. Kamachi, *Polym. J.*, 1994, **26**, 1019–1026.

10 (*a*) C. Rodriguez-Tenreiro, C. Alvarez-Lorenzo, A. Rodriguez-Perez, A. Concheiro and J. J. Torres-Labandeira, *Eur. J. Pharm. Biopharm.*, 2007, **66**, 55–62; (*b*) Y. Okumura and K. Ito, *Adv. Mater.*, 2001, **13**, 485–487; (*c*) K. Ito, *Polym. J.*, 2007, **39**, 489–499; (*d*) J. Araki and K. Ito, *Soft Matter*, 2007, **3**, 1456–1473; (*e*) T. Oku, Y. Furusho and T. Takata, *Angew. Chem., Int. Ed.*, 2004, **43**, 966–969.

11 (*a*) A. Harada, Y. Takashima and H. Yamaguchi, *Chem. Soc. Rev.*, 2009, **38**, 875–882; (*b*) A. Miyawaki, Y. Takashima, H. Yamaguchi and A. Harada, *Tetrahedron*, 2008, **64**, 8355–8361.

12 (*a*) W. Deng, H. Yamaguchi, Y. Takashima and A. Harada, *Angew. Chem., Int. Ed.*, 2007, **46**, 5144–5147; (*b*) W. Deng, H. Yamaguchi, Y. Takashima and A. Harada, *Chem.–Asian J.*, 2008, **3**, 687–695.

13 (*a*) T. Taira, Y. Suzaki and K. Osakada, *Chem. Eur. J.*, 2010, **16**, 6518–6529; (*b*) T. Taira, Y. Suzaki and K. Osakada, *Chem. Commun.*, 2009, 7027–7029.

14 (*a*) L. X. Jiang, Y. Peng, Y. Yan, M. L. Deng, Y. L. Wang and J. B. Huang, *Soft Matter*, 2010, **6**, 1731–1736; (*b*) L. X. Jiang, Y. Peng, Y. Yan and J. B. Huang, *Soft Matter*, 2011, **7**, 1726–1731; (*c*) Y. Yan, L. X. Jiang and J. B. Huang, *Phys. Chem. Chem. Phys.*, 2011, **13**, 9074–9082.

15 (*a*) N. Sreenivasachary and J. M. Lehn, *Proc. Natl. Acad. Sci. U. S. A.*, 2005, **102**, 5938–5943; (*b*) A. Brizard, M. Stuart, K. van Bommel, A. Friggeri, M. de Jong and J. van Esch, *Angew. Chem., Int. Ed.*, 2008, **47**, 2063–2066.